Ternary Hypervalent Silicon Hydrides via Lithium at High Pressure

Tianxiao Liang,[1] Zihan Zhang,[1] Xiaolei Feng,[2,3,*] Haojun Jia,[4]
Chris J. Pickard,[5,6] Simon A. T. Redfern,[7,8] and Defang Duan[1,†]

[1] *College of Physics, Jilin University, Changchun 130012, China*
[2] *Institute for Disaster Management and Reconstruction, Sichuan University - the Hong Kong Polytechnic University, Chengdu, China, 610207*
[3] *Department of Earth Science, University of Cambridge, Downing Site, Cambridge CB2 3EQ, United Kingdom*
[4] *Department of Chemistry, Massachusetts Institute of Technology, Cambridge, Massachusetts 02139, USA*
[5] *Department of Materials Science & Metallurgy, University of Cambridge, 27 Charles Babbage Road, Cambridge CB3 0FS, United Kingdom*
[6] *Advanced Institute for Materials Research, Tohoku University 2-1-1 Katahira, Aoba, Sendai, 980-8577, Japan*
[7] *Asian School of the Environment, Nanyang Technological University, Singapore 639798*
[8] *Center for High Pressure Science and Technology Advanced Research, Beijing 100094, China*

Hydrogen is rarely observed as ligand in hypervalent species, however, we find that high-pressure hydrogenation may stabilise hypervalent hydrogen-rich materials. Focussing on ternary silicon hydrides via lithium doping, we find anions composed of hypervalent silicon with H ligands formed under high pressure. Our results reveal two new hypervalent anions: layered-SiH_5^- and tricapped triangular prismatic SiH_6^{2-}. These differ from octahedral SiH_6^{2-} described in earlier studies. In addition, there are further hydrogen-rich structures, Li_3SiH_{10} and $Li_2SiH_{6+\delta}$, which may be stabilised at high pressure. Our work provides pointers to future investigations on hydrogen-rich materials.

I. INTRODUCTION

Hypervalences are well established in chemistry, referring to aggregates, such as molecules, ions, hydrogen bonds, and other extended structures, in which main group atoms, as a result of their coordination with ligands, adopt a valence electron configuration that exceeds eight [1]. The electronegativity of hydrogen is similar to that of p-block element central atoms, and this explains why hydrogen is rarely observed as ligand in hypervalent species [2]. Linear bonding in hypervalent species is visually described by the three-center-four-electron ($3c-4e$) model [3–5] and it is generally acknowledged that a high polarity is essential to stabilize a hypervalent bond. The Lewis-Langmuir theory of valence attributes the stability of molecules to their ability to place their valence electrons, which appropriately paired off as chemical bonds into stable octets [6, 7]. This theory can be said to have survived the advent of quantum mechanics, with the electron-pairs being replaced by doubly-occupied molecular orbitals or approximately-localized bond orbitals, and with the "cubical atom" being replaced by the directed valences of p-bonds, so that undistorted bonds form along perpendicular axes rather than towards the corners of tetrahedra.

Some previous theoretical and experimental studies show that the alkali metal potassium(K) can form K-Si-H compounds, in which potassium silyl $KSiH_3$ exhibits a high hydrogen content of 4.1 $wt\%$ and maintains an excellently reversible reaction without any disproportionation through direct hydrogenation of the KSi Zintl phase near 130 °C and ambient pressure, consistent with theoretical calculations [8–11]. In 2012, K_2SiH_6 with a cubic $Fm\overline{3}m$ structure was synthesized via reactions of $K_2SiH_6 \rightarrow 2KH + Si + 2H_2$ and $K_2SiH_6 \rightarrow K + KSi + 3H_2$ at pressures above 4 GPa and temperatures between 450 and 650 °C. This phase contains octahedral SiH_6^{2-} and additional hypervalences of the central Si atoms [12]. We believe that there should be similar additional hypervalences for central Si atoms when combined with alkali metal hydrides at high pressure.

In this work, the alkali metal lithium (Li) was chosen to form Li-Si-H compounds. Here, the atomic mass of lithium is relatively light such that it enhances the hydrogen content to achieve the same stoichiometric ratio to metal as seen in K_2SiH_6 and similar compounds. In addition, we explore new ternary phases and investigate their peculiar structures and properties at high pressure, and find that these potential structures may be stableat ambient pressure.

II. COMPUTATIONAL DETAILS

Full variable-composition predictions for Li-Si-H system were firstly performed within 15,000 structures using the ab initio random structure searching approach (AIRSS) [13, 14] at pressures of 1 atm, 50 GPa, 100 GPa, and 200 GPa. Then, fixed composition predictions were employed to further search structures for stable compounds by means of the AIRSS code. The CASTEP code [15] was also used for the structure searches. The VASP (Vienna ab initio simulation packages) code [16] was used to optimize crystal structures and calculate the electronic properties, where the Perdew–Burke–Ernzerhof (PBE) [17] generalized gradient approximation (GGA)

* xf232@cam.ac.uk
† duandf@jlu.edu.cn

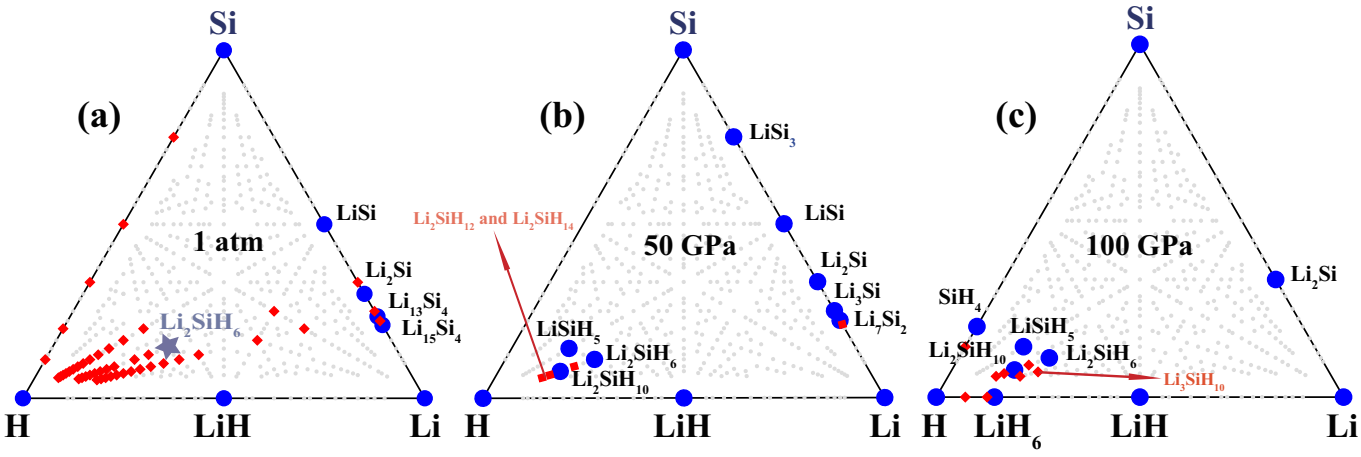

FIG. 1. The ternary phase diagram of Li-Si-H at (a) 1 atm, (b) 50 GPa, and (c) 100 GPa. Large filled blue circles represent which located on the phase diagrams, and small red diamonds represent which didn't locate on the phase diagrams. A metastablestructure with a ratio of Li_2SiH_6 is marked in star in (a), which is dynamically stable.

[18] with the projector-augmented wave method (PAW) [19] was performed. The $1s^1$, $1s^22s^1$ and $2s^22p^63s^23p^2$ configurations were treated as valence electrons for H, Li and Si, respectively. The kinetic cutoff energy of 800 eV, and Monkhorst-Pack $\boldsymbol{k}$ meshes with grid spacing of $2\pi \times 0.03\mathring{A}^{-1}$ were then adopted to ensure enthalpy convergence to less than 1 meV/atom. Phonon calculations were performed in the PHONOPY code [20] to explore dynamic stability of the proposed structures. To investigate the Si-H bonding characteristics, the ICOHPs were calculated as implemented in the LOBSTER [21] package, which provides an atom-specific measure of the bonding character of states in a given energy region.

III. RESULTS AND DISCUSSIONS

We performed a full structure search of the ternary composition space bounded by Li-Si-H at 1 atm, 50 GPa and 100 GPa using the AIRSS code, which enabled us to construct a ternary phase, given in Fig 1. The compounds located on the convex hull are thermodynamically stable when their enthalpy of formation is negative relative to the elements and any other compound. The ternary phase diagram is determined using the convex hull construction. From the ternary phase diagram in Fig.1, we have identified several new stable and metastable stoichiometries, including $LiSiH_5$, Li_2SiH_6, Li_2SiH_{10}, and $Li_2SiH_{6+\delta}$, $\delta = 4, 6, 8$. The crystal structures of these new Li-Si-H compounds are shown in Fig.2, and their structural parameters and atomic coordinates are listed in Table S1 in the supplementary material (SM). These results provide important pointers towards the searching for synthesis of new ternary hydrogen-rich metal hydrides.

As shown in Fig. 1, there are no stable ternary compounds located on the convex hull at 1 atm. It is interesting that $LiSiH_5$, Li_2SiH_6, and Li_2SiH_{10} denoted as large filled blue circles appear on the convex hull in our calculations at 50 and 100 GPa, indicating these ternary hydrides can be stabilized by increased pressure. In addition, the enthalpies of formation of Li_3SiH_{10}, Li_2SiH_{12}, and Li_2SiH_{14} are less than 2 meV/atom above the convex hull at 50 GPa or 100 GPa, and thus these compounds are assumed to be potentially metastable. We also performed variable-composition predictions at 200 GPa, but all ternary compounds move off the convex hull, by more than 0.3 eV/atom, as shown in Fig S 1 in the SM. So, below we confine our discussion to the structure and properties of the predicted stable and metastable compounds below 200 GPa.

For the stoichiometry $LiSiH_5$, we obtain two thermodynamically stable structures in space groups $P2_1c$ and $P2_12_12$ with folded layer-typed SiH_5^- ions (Fig S 2 in the SM). Our phonon calculations, however, show that there are too many imaginary frequencies across the whole Brillion zone suggesting they are dynamically unstable (Fig S 3 in the SM). We identify a metastable structure with space group $R32$ which has an enthalpy just slightly higher than that of the$P2_1c$ and $P2_12_12$ phases, and is dynamically stable over the pressure range of 60 $\sim$ 150 GPa (Fig S 4 and S 5 in the SM). This structure contains flat layer-typed SiH_5^- ions, with Li atoms filling in Si-H layers, (Fig S 6(b) in the SM). This is the first such configuration found as an inorganic structure, and is different from the SiH_5^- previously identified in EtSiH through the

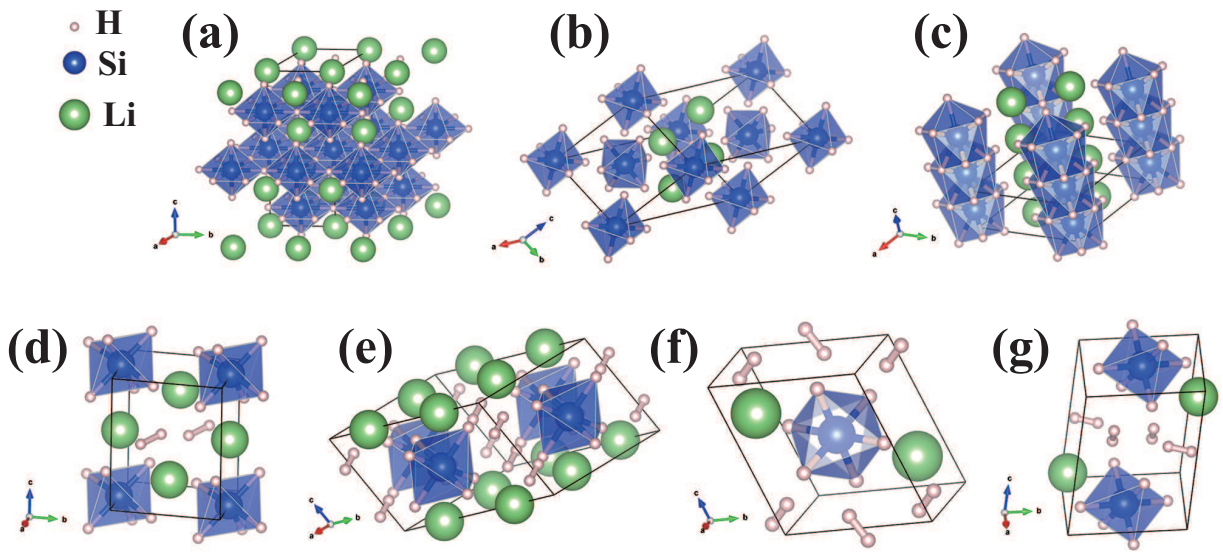

FIG. 2. Crystal structures of Li-Si-H ternary compounds, which are (a) $R32$_$LiSiH_5$ at 100 GPa, (b) $P2_1c$_Li_2SiH_6 at 50 GPa, (c) $P\bar{6}2m$_Li_2SiH_6 at 1 atm, (d), (e), (f) and (g) are $P\bar{1}$_Li_3SiH_{10}, $C2/m$_Li_2SiH_{10}, $P\bar{1}$_Li_2SiH_{12} and $P\bar{1}$_Li_2SiH_{14} at 100 GPa. There are 1 type of SiH_5^- in layers, and 2 types of SiH_6^{2-}, which are originally octahedral ions or tricapped triangular prismatic ions.

chemical reaction of $Et_3SiH_2^- + SiH_4 \rightarrow SiH_5^- + Et_3SiH$ in earlier studies [22]. The only hypervalent all-hydride species reported before is the SiH_5^- ion, which was identified by mass spectrometry [23] as a product of the gas phase ion–molecule reaction. That form of SiH_5^- ion has been reported stable with respect to the loss of H^-, but unstable with respect to decomposition into SiH_3^- and H_2 [24–26]. SiH_5^- in $EtSiH_5$ is composed of one axial H-Si-H unit with 3 H ligands perpendicular to the axial H-Si-H [25]. For the $R32$-type $LiSiH_5$, the upper Si-H layer moves $\frac{2}{\sqrt{3}}d_{\text{Si-H}}$ from lower layers in the crystal lographic direction [210] in $R32$-type $LiSiH_5$ such that $d_{\text{Si-H}}$ is the distance between central the Si to the H on the $6c$ site (H on the Si-H plane), and the $R32$ phase conforms to the $3c-4e$ model with 4 H-Si-H units per central Si atom (Fig S 6(a) and (b) in the SM). One H-Si-H is axial and the others lie on the Si-H plane. We can assume that this layer-type SiH_5^- is composed of single $EtSiH_5$-type SiH_5^- ions in the $R32$-type $LiSiH_5$, and Li atoms are filled between Si-H layers. We should note that the $3c-4e$ model does not explain why Si atoms can accommodate significant ligands in their valence shell, although it accounts for the bonding in hypervalent species.

The stoichiometry Li_2SiH_6 adopts the structure $P2_1c$ at low pressure, which transforms into a $P\bar{6}2m$ phase at 110 GPa (Fig S 7 in the SM). For $P2_1c$-type Li_2SiH_6, the original hypervalent octahedral structure SiH_6^{2-} is favored, obeying the $3c-4e$ model. We have identified new tricapped triangular prismatic SiH_6^{2-} in the $P\bar{6}2m$-type Li_2SiH_6. There are three H atoms surrounding each Si atoms lying parallel to crystal face (001) with 120° angles, in a planar triangular configuration. Two Si atoms are connected by three more H atoms forming a Si-H triangular prism. Si atoms expand three unique H atoms, and share six H atoms with neighbouring Si atoms to form tricapped triangular prismatic SiH_6^{2-} ions. Li atoms are filled in line in $P\bar{6}2m$-type Li_2SiH_6. Finally, we calculated the phonon spectra of $P2_1c$ and $P\bar{6}2m$ phases at different pressures, as shown in Fig.3 and Fig S 8 in the SM. The absence of phonons lying at imaginary frequencies in the phonon spectra indicates that the $P2_1c$-type Li_2SiH_6 is dynamically stable between 50 and 100 GPa. $P\bar{6}2m$-type Li_2SiH_6 is dynamically stable over the pressure range $0 \sim 150$ GPa, (Fig S 8 in the SM).

For the high hydrogen content Li_2SiH_{10}, the $C2/m$ structure is favored and this structure contains original octahedral-structured SiH_6^{2-} units, as shown in Fig.2(e). In this structure, Li atoms and octahedral-structured SiH_6^{2-} ions are staggered and H_2 molecular units fill in the gaps. Furthermore, our phonon calculations show that $C2/m$-type Li_2SiH_{10} is dynamically stable over the pressure range $10 \sim 100$ GPa, (Fig S 9 in the SM).

Additional metastable compounds that we identify comprise Li_3SiH_{10}, Li_2SiH_{12}, and Li_2SiH_{14}, and adopt space group $P\bar{1}$. These all contain original octahedral-structured SiH_6^{2-} units and H_2 units. A variety of Si-H bonds oriented in different directions exist with H_2 units and these are extended into different directions in these structures, which reduces the symmetries of these compounds to triclinic or monoclinic. Phonon calculations show that Li_3SiH_{10} is stable at the pressure range of $70 \sim 100$ GPa, Li_2SiH_{12} is stable at the pressure range of $50 \sim 100$ GPa, and Li_2SiH_{14} is stable at the pressure range of $50 \sim 150$ GPa (Fig S 10 $\sim$ Fig S 12 in the SM).

We have examined the electronic properties of our new

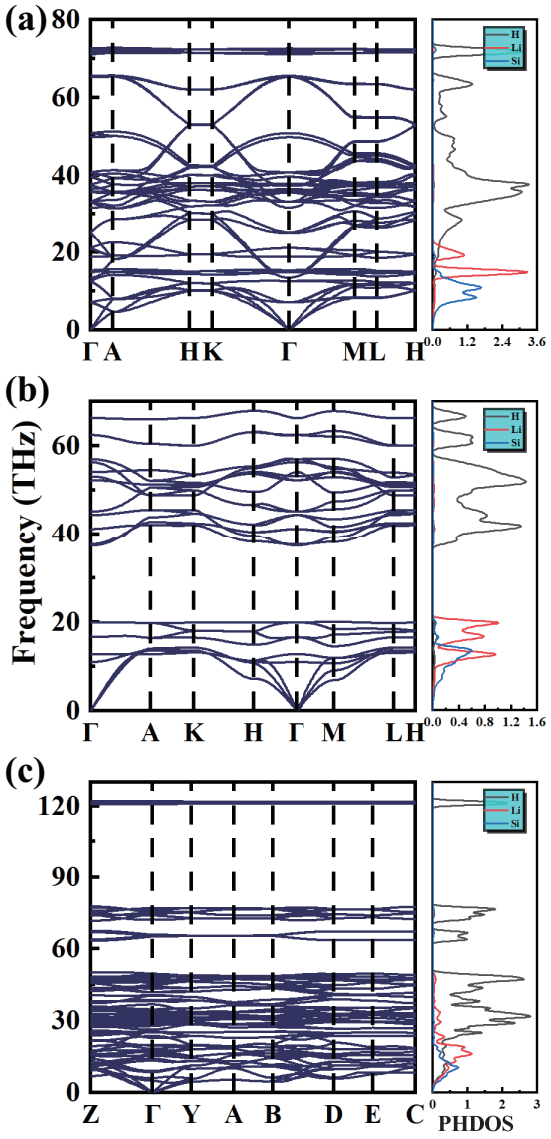

FIG. 3. Calculated phonon dispersion relations (left panel) and densities of the phonon states (right panel) of (a) $R32$_LiSiH$_5$, (b) $P\bar{6}2m$_Li$_2$SiH$_6$, and (c) $C2/m$_Li$_2$SiH$_{10}$ at 100 GPa.

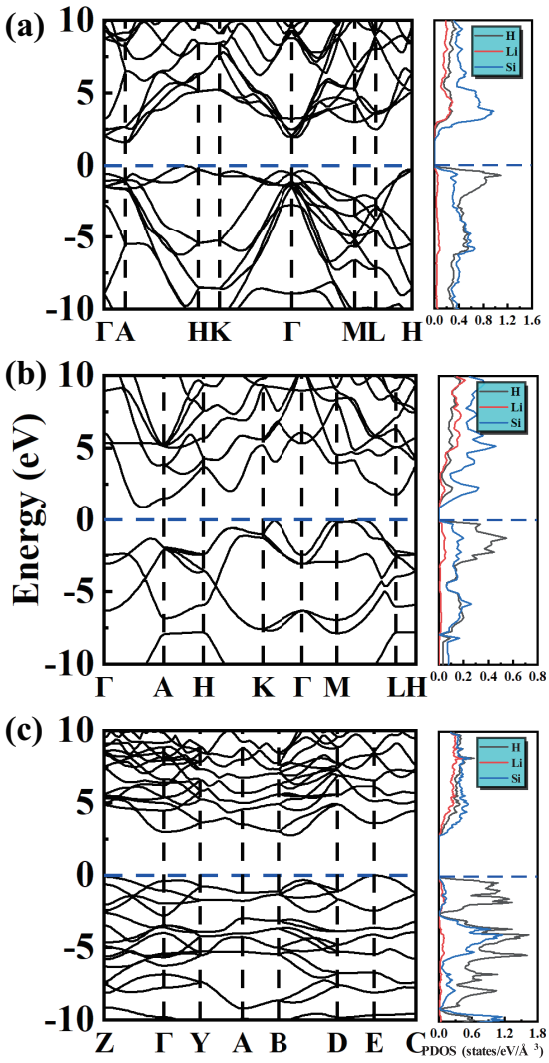

FIG. 4. Calculated band structure (left panel) and projected density of states (right panel) of (a) $R32$_LiSiH$_5$ at 100 GPa, (b) $P\bar{6}2m$_Li$_2$SiH$_6$ at 1 atm, and (c) $C2/m$_Li$_2$SiH$_{10}$ at 10 GPa. The Fermi level is set to zero and depicted as the blue dash line.

Li-Si-H compounds based on their equilibrium crystal structures. The Bader charge analysis [27] was used to determine charge transfer, and the electron localization function (ELF) [28] was used to describe and visualize chemical bonds in molecules and solids. Bader charge analysis reveals charge transfer from Li/Si to H, as listed in Table S2 in the SM, suggesting that both Li and Si are electron donors and provide electrons to H atoms. For all the stable phases, Li consistently loses approximate 0.8 $\sim$ 0.9e, and Li-ions form ionic bonds with Si-H anions. Furthermore, from the ELF in Fig S 13, we confirm the ionic bonding nature of Li-ions in view of the absence of charge localization between Li and other elements, and weak covalent Si-H bonding via the observation of charge localization between the nearest-neighbor Si and H atoms. Moreover, in $C2/m$-type Li$_2$SiH$_{10}$, there are a lot of H$_2$ molecular units which is evident by strong charge localization between the nearest-neighbor H atoms.

The electronic band structures and projected density of states (DOS) for the predicted stable and metastable structures have also been explored and are presented in Fig.4 and Fig S 14 $\sim$ S 18 in the SM. One can see that most of Li-Si-H compounds have large-band gaps, greater than 1.0 eV, indicating that the majority of these Li-Si-H compounds are insulators except for $P\bar{1}$-type Li$_3$SiH$_{10}$. There are few bands across the Fermi level and the values of DOS at the Fermi level is small for the $P\bar{1}$-type Li$_3$SiH$_{10}$ suggesting it is a poor electrical conductor, as shown in Fig S 18.

We here propose a generally useful system to designate the bonding around the Si atoms. Such a bonding system

TABLE I. The ICOHPs for Si-H bonding in $LiSiH_5$, Li_2SiH_6, and Li_2SiH_{10} at different pressures.

Hydrides	Pressure (GPa)	Bond length ($\AA$)	ICOHP (eV)	Bonding types
$LiSiH_5$ $R32$	100	1.46	−1.97	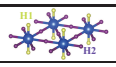
		1.62	−2.07	
Li_2SiH_6 $P\bar{6}2m$	50	1.75	−1.19	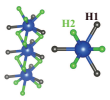
		1.79	−0.44	
	100	1.62	−1.65	
		1.67	−1.51	
Li_2SiH_{10} $C2/m$	50	1.51	−1.52	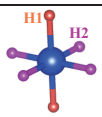
		1.53	−2.73	
	100	1.46	−2.06	
		1.49	−3.01	

is described as an N-X-L system [29]. N represents the number of total valence electrons, X is central atom, Si in our case, and L is the number of ligand atoms. There are three different such systems which can be thus designated. The first is $10-\mathrm{Si}-8$ $R32$-type $LiSiH_5$, which is thus different to the $10-\mathrm{Si}-5$ seen in $EtSiH_5$ [22]. Additionally we identify $12-\mathrm{Si}-9$ for $P\bar{6}2m$-type Li_2SiH_6, and $12-\mathrm{Si}-6$ for $Li_2SiH_{6+\delta}$ and $P\bar{1}$-Li_3SiH_{10}.

As mentioned above, the bonding between the H and Si atoms is covalent, composing hypervalent silicic anions SiH_5^- or SiH_6^{2-}, which are strong and hard to disrupt at high pressure, as seen when we combine our data with the integrated crystalline orbital Hamiltonian population (ICOHP) [30] results in Table I. For various ICOHP values, stronger Si-H bonds give larger negative values. There are two types of Si-H bonds in $R32$-type $LiSiH_5$: one is Si-H1 bonding in the flat layer with distance of 1.46 $\AA$, the other is Si-H2 bonding perpendicular to the flat layer with distance of 1.62 $\AA$. The integrated ICOHP up to the Fermi levels are -2.08 eV for Si–H1 bonding, and -1.97 eV for Si–H2 bonding in the $R32$-type $LiSiH_5$ at 100 GPa. As for $P\bar{6}2m$-type Li_2SiH_6, there are two types Si-H bonding in tricapped triangular prismatic SiH_6^{2-} as well. Each of Si atoms expands three H1 atoms involving iSi-H1 bonding with a distance of 1.67 $\AA$. Another interaction is Si-H2 bonding with distance of 1.62 $\AA$, and two Si atoms are connected to three H2 atoms forming the Si-H2 triangular prism. The ICOHP up to Fermi levels are -1.51 eV for Si-H1, and -1.65 eV for Si-H2 at 100 GPa. For $P2_1c$-type Li_2SiH_6, $Li_2SiH_{6+\delta}$, and $P\bar{1}$-Li_3SiH_{10}, there is only one type of Si-H bond in octahedral-structured SiH_6^{2-} ions. But there is a pair of Si-H bonding in longer bond lengths but more negative ICOHP values to Fermi levels. For $C2/m$-type Li_2SiH_{10}, a pair of Si-H1 bond lengths lie at 1.49 $\AA$, and another two pairs of Si-H2 bond lengths are 1.46 $\AA$ at 100 GPa. It is interesting that Si-H1 with longer bond length tends to be more stable and harder to break at high pressure. These results suggest that the Si–H bonds in anions SiH_5^- or SiH_6^{2-} are strongly covalent at high pressure and prove hard to eliminate.

It is found that all the predicted compounds have high gravimetric hydrogen contents and volumetric hydrogen densities, suggesting that they may be potential hydrogen storage materials. The $P\bar{6}2m$-type Li_2SiH_6, at ambient pressure, has a very high volumetric hydrogen density of 175.04 g/L with 12.51$wt\%$ theoretical gravimetric hydrogen content. Moreover, $P\bar{1}$-type Li_2SiH_{14} has the highest volumetric hydrogen density of 352.31 g/L, with 25.02 $wt\%$ theoretical gravimetric hydrogen content. We plot the values of these hydrogen densities in Fig S 19 in the SM.

IV. CONCLUSIONS

In summary, we have explored the crystal structures and stabilities of compounds within the Li-Si-H ternary system under high pressure by employing *ab initio* calculations as implemented in the AIRSS random structure search method. We predict the existences of several hydrogen-rich structures at high pressures, including $R32$-type $LiSiH_5$, $P\bar{6}2m$-type Li_2SiH_6, and $C2/m$-type Li_2SiH_{10}. Furthermore, we find highly hydrogen-rich structures in the form of $P\bar{1}$-type Li_2SiH_{12}, $P\bar{1}$-type Li_3SiH_{10} and $P\bar{1}$-type Li_2SiH_{14}, which accommodate high hydrogen content in the form of H_2 units inside. We find two new types of hypervalent ions. One of them is layer-typed SiH_5^- in $R32$-type $LiSiH_5$ containing 4 H-Si-H units per central Si atom, one is axial and others comprise the 2-D layers. The other variety of hypervalent ion that we identify is tricapped triangular prismatic SiH_6^{2-} in $P\bar{6}2m$-type Li_2SiH_6. This does not obey the $3c-4e$ model and dynamically stableat both ambient pressure and high pressure. The prediction of tricapped triangular prismatic SiH_6^{2-} may be a new challenge to the $3c-4e$ model. Based on our results we propose a new method for designing novel ternary hydrogen rich materials. We believe that our work provides useful guidance and waymarkers for future experimental synthesis of ternary alkali and alkaline earth metal hydrides.

ACKNOWLEDGMENTS

This work was supported by National Natural Science Foundation of China (Nos. 11674122 and 11704143). X. Feng acknowledges China Scholarship Council. CJP acknowledges financial support from the Engineering and Physical Sciences Research Council [Grant EP/P022596/1] and a Royal Society Wolfson Research Merit award. Parts of calculations were performed in the High Performance Computing Center (HPCC) of Jilin University and TianHe-1(A) at the National Supercomputer Center in Tianjin.

[1] S. Noury *et al*, Chemical bonding in hypervalent molecules: is the octet rule relevant? Inorg. Chem. **41**, 2164–2172 (2002).

[2] P. Treichel *et al*, Synthesis and characterization of HPF_4 and H_2PF_3, J. Am. Chem. Soc. **89**, 2017–2022 (1967).

[3] R. J. Hach *et al*, The structure of tetramethylammonium pentaiodide[1,1a], J. Am. Chem. Soc. **73**, 4321–4324 (1951).

[4] G. C. Pimentel, The bonding of trihalide and bifluoride ions by the molecular orbital method, J. Chem. Phys. **19**, 446–448 (1951).

[5] V. B. Koutecký *et al*, A molecular orbital description for sulfur compounds of valences 2, 4 and 6, Theo. Chim. Acta. **33**, 227–238 (1974).

[6] G. N. Lewis, The atom and the molecule, J. Am. Chem. Soc. **38**, 762–785 (1916).

[7] I. Langmuir, The arrangement of electrons in atoms and molecules, J. Am. Chem. Soc. **41**, 868–934 (1919).

[8] R. Janot *et al*, Catalyzed $KSiH_3$ as a reversible hydrogen storage material, J. Mater. Chem. A **4**, 19045–19052 (2016).

[9] J. N. Chotard *et al*, Potassium silanide ($KSiH_3$): A reversible hydrogen storage material, Chem-Eur. J. **17**, 12302–12309 (2011).

[10] M. A. Ring *et al*, Preparation and reactions of potassium silyl[1], J. Am. Chem. Soc. **83**, 802–805 (1961).

[11] M. Ring *et al*, Crystal structure of potassium silyl, J. Phys. Chem. **65**, 182–183 (1961).

[12] K. Puhakainen *et al*, Hypervalent octahedral SiH_6^{2-} species from high-pressure synthesis, Angew. Chem. Int. Ed. Engl. **51**, 3156–3160 (2012).

[13] C. J. Pickard *et al*, Ab initio random structure searching, J. Phys. Condens. Matter. **23**, 053201 (2011).

[14] C. J. Pickard *et al*, High-pressure phases of silane, Phys. Rev. Lett **97**, 045504 (2006).

[15] M. Segall *et al*, First-principles simulation: ideas, illustrations and the castep code, J. Phys. Condens. Matter. **14**, 2717 (2002).

[16] G. Kresse *et al*, Efficiency of ab-initio total energy calculations for metals and semiconductors using a plane-wave basis set, Comput. Mater. Sci. **6**, 15-50 (1996).

[17] J. P. Perdew *et al*, Generalized gradient approximation made simple, Phys. Rev. Lett **77**, 3865 (1996).

[18] J. P. Perdew *et al*, Pair-distribution function and its coupling-constant average for the spin-polarized electron gas, Phys. Rev. B **46**, 12947 (1992).

[19] P. E. Blöchl, Projector augmented-wave method, Phys. Rev. B **50**, 17953 (1994).

[20] A. Togo *et al*, First-principles calculations of the ferroelastic transition between rutile-type and $CaCl_2$-type SiO_2 at high pressures, Phys. Rev. B **78**, 134106 (2008).

[21] V. L. Deringer *et al*, Crystal orbital hamilton population (COHP) analysis as projected from plane-wave basis sets, J. Phys. Chem. A **115**, 5461–5466 (2011).

[22] D. J. Hajdasz *et al*, Hypervalent silicon hydrides: SiH_5, J. Am. Chem. Soc. **108**, 3139–3140 (1986).

[23] J. Sheldon *et al*, Gas-phase ion chemistry of ambident nucleophiles. the methoxide and trifluoromethoxide negative ions reactions with organosilanes and carbonyl compounds: an ab initio and ion cyclotron resonance study, New. J. Chem. **8** 79–85 (1984).

[24] T. Taketsugu *et al*, Dynamic reaction path study of sih4+ h-. fwdarw. sih5-and the berry pseudorotation mechanism, J. Phys. Chem. **99**, 14597–14604 (1995).

[25] S. C. Pierrefixe *et al*, Hypervalence and the delocalizing versus localizing propensities of H_3^-, Li_3^-, CH_5^- and SiH_5^-, Struct. Chem. **18**, 813–819 (2007).

[26] S. C. Pierrefixe *et al*, Hypervalent silicon versus carbon: Ball-in-a-box model, Chem-Eur. J. **14**, 819–828 (2008).

[27] R. Bader, Atoms in molecules, Acc. Chem. Res. **18**, 9 (1985).

[28] A. D. Becke *et al*, A simple measure of electron localization in atomic and molecular systems, J. Chem. Phys. **92**, 5397–5403 (1990).

[29] C. Perkins *et al*, An electrically neutral. sigma.-sulfuranyl radical from the homolysis of a perester with neighboring sulfenyl sulfur: 9-S-3 species, J. Am. Chem. Soc. **102**, 7753–7759 (1980).

[30] R. Dronskowski *et al*, Crystal orbital hamilton populations (COHP): energy-resolved visualization of chemical bonding in solids based on density-functional calculations, J. Phys. Chem. **97**, 8617–8624 (1993).